Ground Penetrating Radar (GPR) Study Over Specific Medium

Marwan
Lecturer, Geophysics Section, Department of Physics, Faculty of Sciences, Syiah Kuala University, Banda Aceh, Indonesia
e-mail: marwan.fisika@gmail.com

Rosli Saad
Senior Lecturer (Dr.), Geophysics Section, School of Physics, Universiti Sains Malaysia, Penang, Malaysia
e-mail: rosli@usm.my

Muhammad Syukri
Senior Lecturer (Dr.), Geophysics Section, Department of Physics Faculty of Sciences, Syiah Kuala University, Banda Aceh, Indonesia
e-mail: m.syukri@unsyiah.ac.id

ABSTRACT

The research was conducted to study the EM velocity in medium. Three studies were conducted, two was in the laboratory and one was on the original ground with known depth and target object. The study indicates that GPR is medium and EM velocity dependent.

KEYWORDS: GPR, EM wave, medium

INTRODUCTION

Ground penetrating radar (GPR) is a high resolution electromagnetic technique designed primarily to investigate the shallow subsurface of the earth, building materials, and roads and bridges (Annan and Davis, 1978; Olhoeft, 1992; Daniels et al., 1998). It is developed for high resolution investigations of the subsurface with time-dependent geophysical technique. The results provide an accurate depth estimates for many common subsurface objects including defining the size, shape, orientation and material properties of buried objects (Roberts, 1994; Roberts and Daniels, 1996; 1997). It has also proven to be a tool that can be operated in boreholes to extend the range of investigations away from the boundary of the hole. The basic principles used were the scattering of electromagnetic (EM) wave with moving antennas over the surface rather than rotating about a fixed point. This has led to the application of field operational principles that are analogous to the seismic reflection method. GPR is a method that is commonly used for environmental, engineering, archeological, and other shallow investigations.

BASIC THEORY

A GPR system consists of a few components, transmitter that emits an EM wave into the ground and receives the response by receiver (Figure 1). If there is a change in electric properties in the ground or if there is an anomaly that has different electric properties surrounds the media, part of the wave is reflected to the receiver. The GPR profile can be constructed by plotting the amplitude of the received signals as a function of time and position, representing a vertical slice of the subsurface (Figure 2). The time axis can be converted to depth by assuming a velocity for the EM wave in the subsurface soil.

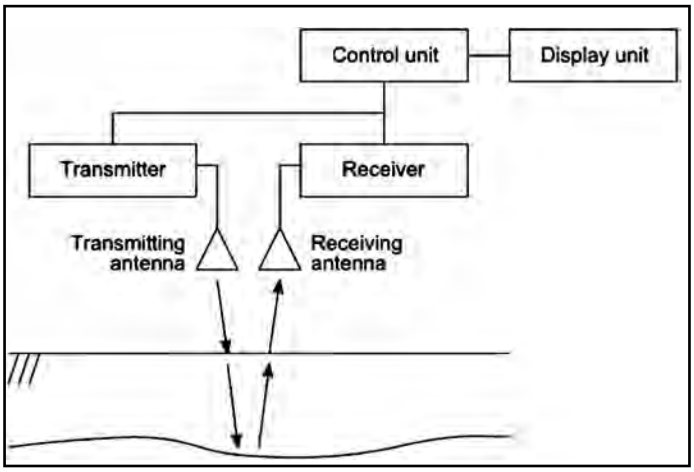

Figure 1: Schematic diagram of GPR system.

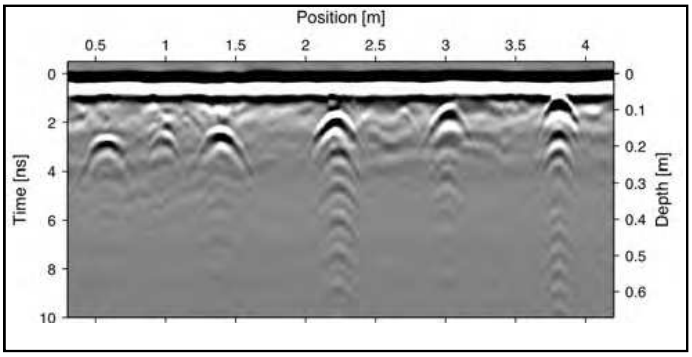

Figure 2: GPR profile obtained with a 1.5 GHz system scanned over six objects buried in sandy soil. The signal amplitude is plotted as a function of time (or depth) and position. Objects are recognized by hyperbolic-shaped reflections. Reflections from the ground surface appear as stripes at the top of the profile.

The propagation velocity v of the electromagnetic wave in soil is characterized by the dielectric permittivity, ε and magnetic permeability, μ of the medium:

$$v = \frac{1}{\sqrt{\varepsilon\mu}} = \frac{1}{\sqrt{\varepsilon_0\varepsilon_f\mu_0\,\mu_f}} \tag{1}$$

where $\varepsilon_o = 8.854 \times 10^{-12}$ F/m is the permittivity of free space, $\varepsilon_r = \varepsilon/\varepsilon_o$ is the relative permittivity (dielectric constant) of the medium, $\mu_o = 4\pi \times 10^{-7}$ H/m is the free-space magnetic permeability, and $\mu_r = \mu/\mu_o$ is the relative magnetic permeability. In most soils, magnetic properties are negligible, yielding $\mu = \mu_o$, and Eq. 1 becomes

$$v = \frac{c}{\sqrt{\varepsilon_r}} \tag{2}$$

where $c = 3 \times 10^8$ m/s is the speed of light. The wavelength, λ is defined as the distance of the wave propagation in one period of oscillation and is obtained by

$$\lambda = \frac{v}{f} = \frac{2\pi}{\omega\sqrt{\varepsilon\mu}} \tag{3}$$

where f is the frequency and $\omega = 2\pi f$ is the angular frequency. In general, dielectric permittivity, ε and electric conductivity, σ is complex and can be expressed as

$$\varepsilon = \varepsilon' - j\varepsilon'' \tag{4}$$

$$\sigma = \sigma' - j\sigma'' \tag{5}$$

where ε' is the dielectric polarization term, ε" represents the energy loss due to the polarization lag, σ' refers to conduction, and σ" is related to diffusion (Knight and Endres, 2005). A complex effective permittivity expresses the total loss and storage effects of the material as a whole (Cassidy, 2009):

$$\varepsilon^{c} = \left(\varepsilon' + \frac{\sigma''}{\omega}\right) - j\left(\varepsilon'' + \frac{\sigma'}{\omega}\right) \tag{6}$$

The ratio of the imaginary and real parts of the complex permittivity is defined as tan δ (loss tangent):

$$\tan\delta = \frac{\varepsilon''}{\varepsilon'} \cong \frac{\sigma'}{\omega\varepsilon'} \tag{7}$$

When ε" and σ" are small, it is approximated as the right most expression. In the plane wave solution of Maxwell's equations, the electric field, E of an EM wave that is travelling in z-direction is expressed as

$$E(z,t) = E_0 e^{j(\omega t - kz)} \tag{8}$$

where, E_o is the peak signal amplitude and $k = \omega\sqrt{\varepsilon\mu}$ is the wave number, which is complex if the medium is conductive, and it can be separated into real and imaginary parts:

$$k = \alpha + j\beta \tag{9}$$

The real part, α and imaginary part, β are called the attenuation constant (Np/m) and phase constant (rad/m), respectively, and given as follows:

$$\alpha = \omega\left[\frac{\varepsilon'\mu}{2}\left(\sqrt{1+\tan^2\delta} - 1\right)\right]^{1/2} \tag{10}$$

$$\beta = \omega\left[\frac{\varepsilon'\mu}{2}\left(\sqrt{1+\tan^2\delta}+1\right)\right]^{1/2} \tag{11}$$

The attenuation constant can be expressed in dB/m by α' = 8.686α. The inverse of the attenuation constant:

$$\delta = \frac{1}{\alpha} \tag{12}$$

is called the skin depth. It gives the depth at which the amplitude of the electric field decay is 1/*e* (~ -8.7 dB, ~ 37%). It is a useful parameter to describe how lossy the medium is. Table 1 provides the typical range of permittivity, conductivity and attenuation of various materials.

Table 1: Typical range of dielectric characteristics of various materials measures at 100 MHz (Daniels, 2004; Cassidy, 2009).

Material	Relative permittivity	Conductivity(S/m)	Attenuation constant(dB/m)
Air	1	0	0
Freshwater	81	10^{-6}-10^{-2}	0.01
Clay, dry	2–6	10^{-3}-10^{-1}	10-50
Clay, wet	5-40	10^{-1}-10^{-0}	20-100
Sand, dry	2-6	10^{-7}-10^{-3}	0.01-1
Sand, wet	10-30	10^{-3}-10^{-2}	0.5-5

GPR methods measures reflected or scattered EM waves from changes in the electric properties of materials. Figure 3 shows a planar boundary between two media with different electric properties.

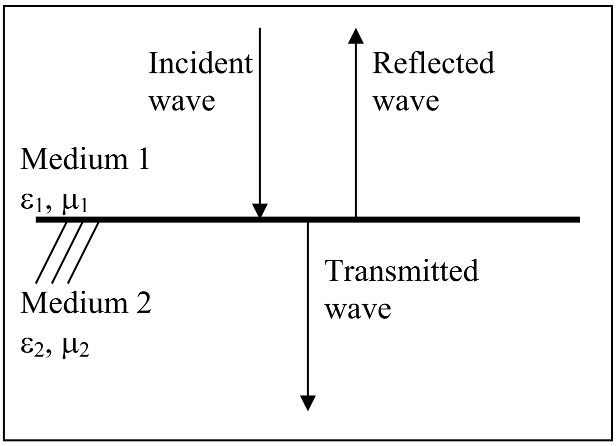

Figure 3: Reflection and transmission of a normal incident EM wave to a planar interface between two media.

When electromagnetic waves hit a planar dielectric boundary, some energy is reflected from the boundary and the remainder is transmitted into the second medium. The relationships of the incident, reflected and transmitted electric field strengths are;

$$Ei = Er + Et \tag{13}$$

$$Er = R.Ei \tag{14}$$

$$Et = T.Ei \tag{15}$$

where, R is the reflection coefficient and T is the transmission coefficient. In the case of normal incidence, the reflection and transmission coefficients are;

$$R = \frac{Z_2 - Z_1}{Z_2 + Z_1} \tag{16}$$

$$T = 1 - R = \frac{2Z_2}{Z_2 + Z_1} \tag{17}$$

where, Z_1 and Z_2 are the intrinsic impedances of the first and second media, respectively, and $Z = \sqrt{\mu\ \varepsilon}$. In a low-loss non-conducting medium, the reflection coefficient is simplified (Daniels, 2004);

$$R \cong \frac{\sqrt{\varepsilon_{r1}} - \sqrt{\varepsilon_{r2}}}{\sqrt{\varepsilon_{r1}} + \sqrt{\varepsilon_{r2}}} \tag{18}$$

The common techniques for soil moisture mapping with GPR is analyzing the ground wave velocity. Surface GPR measures ground wave which the only wave that travels through the ground with known propagation path and the wave velocity can be calculated directly from the traveltime. Analyzing the ground wave has proven to be a fast technique that can be used to map large areas and yield reasonable results in comparison to other methods, such as TDR or gravimetric soil moisture determination (Du, 1996; Grote et al., 2003; Huisman et al., 2001, 2003; Overmeeren et al., 1997).

METHODOLOGY

The research conducted to study the EM wave velocity in a medium. Three studies conducted, two was in the laboratory and one is on the original ground. The laboratory study consists of;

i. the 0.14 m diameter of cylindrical iron pipe was put on the ground. The 500 MHz antenna was run on the top of the cylinder at 0.64 m height with an atmosphere medium (Figure 4a).

ii. the 0.14 m diameter of cylindrical iron pipe was put on the cement surface of a small pool full with water. The 500 MHz antenna was run on the top of the water surface (slightly merge in the water) with 0.48 m from the top of the cylinder (Figure 4b).

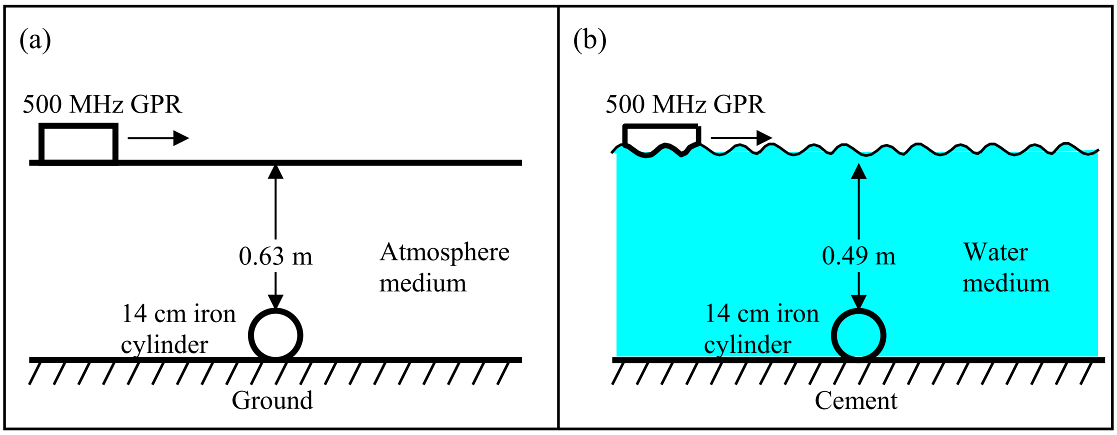

Figure 4: GPR study with 500 MHz antenna for cylinder iron pipe using different medium. (a) Atmosphera (b) Water.

The original ground study conducted at the Universitas Syiah Kuala, Acheh, Indonesia. The target object is a 0.61 m diameter of cylindrical cement drainage buried under the ground with depth of 0.88 m (Figure 5). The GPR data was processed using RAMAC GroundVision and ReflexW software.

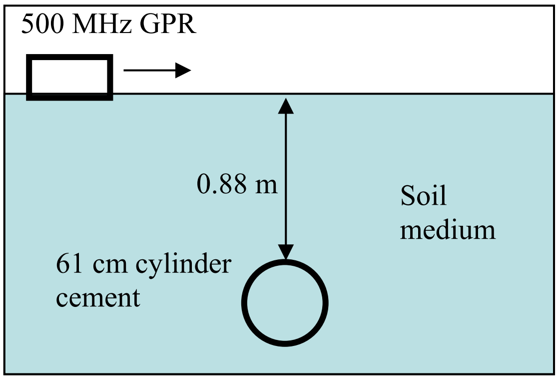

Figure 5: GPR study with 500 MHz antenna for cylinder cement drainage buried in soil medium.

RESULTS AND DISCUSSION

Figure 6a shows GPR profile of the laboratory study of cylindrical iron pipe in atmosphere medium. The profile shows the cylindrical iron pipe was identified at depth of 0.639 m, using EM velocity of 0.3 m/ns. Figure 6b is the GPR profile of cylindrical iron pipe in water medium. The profile shows the cylindrical iron pipe was identified at depth of 0.489 m, using EM velocity of 0.041 m/ns. Figure 7 shows a profile of original ground study for buried cylindrical cement drainage. The profile shows the cylindrical cement drainage was identified at depth of 0.862 m, using EM velocity of 0.115 m/ns. The study indicates that GPR is medium and EM wave velocity dependent.

(a) (b)

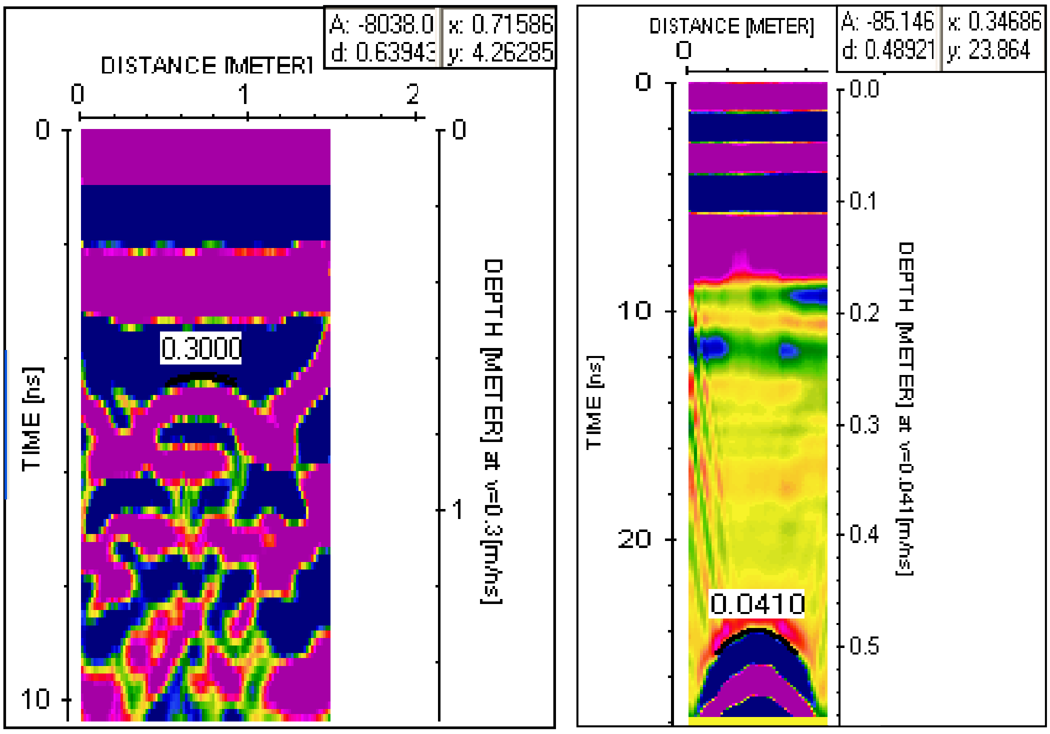

Figure 6: GPR profile obtained with 500 MHz antenna scanned over; (a) a cylindrical iron pipe with an atmosphere medium, (b) a cylindrical iron pipe with water medium. Objects are recognized by hyperbolic-shaped reflections.

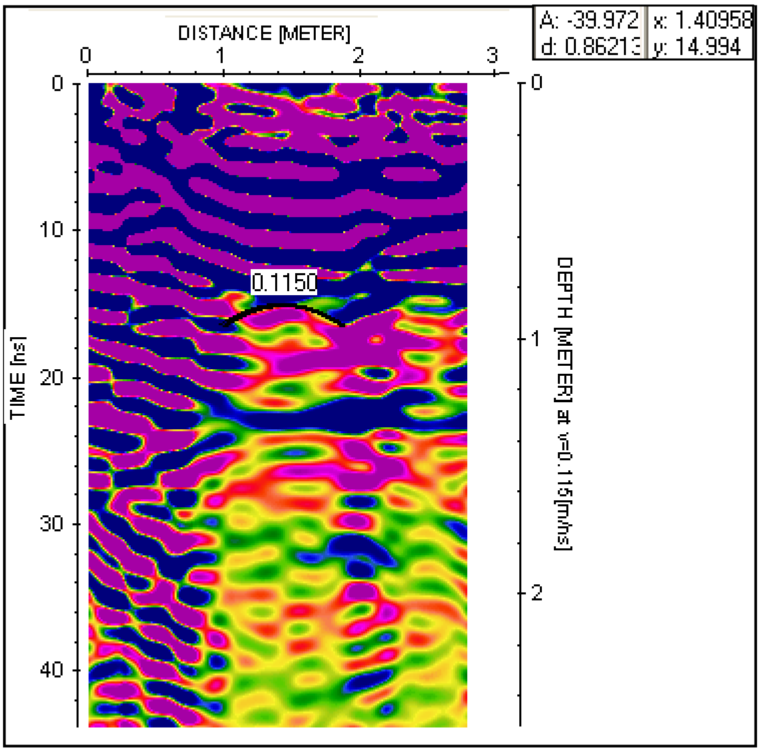

Figure 7: GPR profile obtained with 500 MHz antenna scanned over cylindrical cement drainage. Objects are recognized by hyperbolic-shaped reflections.

CONCLUSSION

The GPR is very useful for shallow subsurface investigate of the earth, building materials, and roads and bridges. It is medium and EM wave velocity dependent.

ACKNOWLEDGEMENTS

Thanking to the Ministry of Education and Culture, Indonesia for financial support in the scheme of Decentralized Research Competitive Grants Program 2014. Special thanks are extended to the technical staffs of the geophysics laboratory and geophysics postgraduate students, School of Physics, Universiti Sains Malaysia and geophysics students, Faculty of Sciences and Faculty of Engineering, Syiah Kuala University for their assistance during the data acquisition.

REFERENCES

1. Annan, A.P. and Davis, J.L., 1978, Methodology for Radar Transillumination Experiments: Report of Activities, Geological Survey of Canada, Paper, 78-1B, pp. 107-110.
2. Cassidy, N.J. (2009). Electrical and magnetic properties of rocks, soils, and fluids, In: Ground Penetrating Radar: Theory and Applications, Jol, H.M., pp. 41-72, Elsevier, ISBN 978-0-444-53348-7, Amsterdam, The Netherlands.
3. Daniels, D.J. (Ed.)., 2004, Ground Penetrating Radar (2nd Edition), IEE, ISBN 0-86341-360-9, London.
4. Daniels, J.J., J. Brower, and F. Baumgartner., 1998, High-resolution GPR at Brookhaven National Laboratory to delineate complex subsurface targets, *J. Environmental & Engineering Geophysics, 3*, 1, 1-6.
5. Du, S., 1996, Determination of Water Content in the Subsurface with the Ground Wave of Ground Penetrating Radar. Dissertation, Ludwig-Maximilians-Universität, München, Germany.
6. Grote, K., Hubbard, S. & Rubin, Y. (2003). Field-scale estimation of volumetric water content using ground-penetrating radar ground wave techniques. Water Resources Research, Vol. 39, pp. 1321-1333.
7. Huisman, J.A., Sperl, C., Bouten, W. & Verstaten, J.M. (2001). Soil water content measurements at different scales: accuracy of time domain reflectometry and ground-penetrating radar. Journal of Hydrology, Vol. 245, pp. 48-58
8. Huisman, J.A., Hubbard, S.S., Redman, J.D. & Annan, A.P. (2003). Measuring soil water content with ground penetrating radar: a review. Vadose Zone Journal, Vol. 2, pp. 476-491
9. Knight, R.J. & Endres, A.L. (2005). An introduction to rock physics principles for nearsurface geophysics, In: Near-Surface Geophysics, Investigations in Geophysics, No.13, Society of Exploration Geophysics, Butler, D.K., pp.357-438, ISBN 1-56080-130-1, Tulsa, OK
10. Olhoeft, G.R., 1992, Data fusion (integration), ch. 3; Ground penetrating radar (GPR), ch. 5, in Workshop on noninvasive geophysical site characterization, Van Eeckhout, E., and Calef, C., compilers: Los Alamos LA-12311-C, UC-903, p. 4-6 and p. 11-14.

11. Overmeeren, R.A., Sariowan, S.V. & Gehrels, J.C. (1997). Ground penetrating radar for determining volumetric soil water content; results of comparative measurements at two test sites. Journal of Hydrology, Vol. 197, pp. 316-338

12. Roberts, R.R., 1994, Analysis and theoretical Modeling of GPR Polarization Data: Ph.D. Dissertation, The Ohio State University, 429 p.

13. Roberts, R.L., and J.J. Daniels, 1996, Analysis of GPR Polarization Phenomena: Journal of Environmental and Engineering Geophysics, vol. 1, No.2, p. 139-157.

14. Roberts, R.L., and J.J. Daniels, 1997, Modeling Near Field GPR in three dimensions using the FDTD Method: Geophysics, Vol. 62, No. 4, p. 1114-1126.